Radicals, Radical Pairs and Triplet States in Photosynthesis

WOLFGANG LUBITZ,*,† FRIEDHELM LENDZIAN,‡ AND ROBERT BITTL§

Max-Planck-Institut für Strahlenchemie, Stiftstrasse 34-36, 45470 Mülheim/Ruhr, Germany, Max-Volmer-Laboratorium für Biophysikalische Chemie, Institut für Chemie, Technische Universität Berlin, Strasse d. 17. Juni 135, 10623 Berlin, Germany, and Institut für Experimentalphysik, Fachbereich Physik, Freie Universität Berlin, Arnimallee 14, 14195 Berlin, Germany

Received July 20, 2001

ABSTRACT

The investigation of radical ions, radical pairs, and triplet states that occur in the primary processes of photosynthesis by various EPR techniques is described. The determination of the valence electron spin density distribution by ENDOR/TRIPLE spectroscopy is demonstrated for the primary electron donor. In combination with site-directed mutagenesis, these studies show that the spin distribution in the chlorophyll donor is strongly affected by the protein environment, and a link is established with the donor's oxidation potential and function in the electron transfer process. Similarities and differences between electron donors in anoxygenic (bacterial) and oxygenic photosynthesis are briefly discussed. Application of transient and pulse EPR techniques give information also on short-lived intermediates, such as radical pairs and triplet states, and allow the determination of distances and relative orientations of these species. The extension to time-resolved pulse ENDOR spectroscopy opens the possibility to resolve the electron−nuclear hyperfine structure of these reaction intermediates, even on a very short time scale.

I. Introduction

Photosynthetic reaction centers (RCs) are considered nature's solar batteries. These integral membrane proteins use sunlight to initiate a fast single-electron transfer (ET) across the photosynthetic membrane. The created potential difference drives subsequent electron and proton transfer reactions, which are coupled to enzymatic reactions that ultimately oxidize water to molecular oxygen and yield strongly reducing compounds needed for the conversion of CO_2 to carbohydrates.[1] Simple green and purple photosynthetic bacteria perform an anoxygenic photosynthesis;[2] they possess only one RC. Cyanobacteria, algae, and green plants are more complex; they utilize two photosystems (PS I and PS II) and perform an oxygenic photosynthesis.[3] Basically, two types of RCs can be distinguished: type I RCs are found in plants as PS I and in green bacteria, whereas type II RCs occur in plants as PS II and in purple bacteria. In all RCs, the cofactors are arranged in two branches. The primary donor (D) is a closely related pair of chlorophyll (Chl) or bacteriochlorophyll (BChl) molecules; the acceptors (A) comprise monomeric chlorophylls, pheophytins (Pheo), and quinones (Q) in type II RCs and chlorophylls, quinones, and iron−sulfur centers in type I RCs. As an example, the basic structure of PS II is shown schematically in Figure 1. It is very similar to the RC of purple bacteria with respect to the chain of acceptors[4,5] but different at the electron donor side, where it harbors a protein-bound manganese cluster, the locus of photosynthetic water oxidation (Figure 1).

The light-induced fast activationless ET proceeds from the singlet excited primary donor D* to a series of acceptors (A_i), as depicted in Figure 2. The process has been studied extensively by fast optical spectroscopy.[6,7] A detailed understanding of the vectorial ET in these RCs clearly requires knowledge of the geometrical and electronic structures of all molecules in all stages of the process. The spatial structure of the purple bacterial RC and of PS I and II has been obtained from X-ray crystallography.[4,5,8] Information on the electronic structure is available from spectroscopy.[9]

EPR is the method of choice to study the paramagnetic intermediates occurring in the reaction sequence.[10] Here the transferred single electron is used as a probe to identify and characterize the species participating in the ET process. The trapped intermediate radical ions are characterized via their electronic *g* factors (Zeeman splitting factor), an approach similar to the use of chemical shifts (of magnetic nuclei) in NMR spectroscopy. To increase the Zeeman resolution and also the sensitivity of the spectra, higher external fields are now being employed.[11] The interaction with internal fields from other unpaired electrons or magnetic nuclei causes line splittings that can be used to determine details of the spatial and electronic structure.

In species with more than one unpaired electron (e.g., triplet states) the electron−electron interaction leads to zero field splitting (ZFS) which contains information about the delocalization of the triplet electons.[10,12] In biradical and radical pair states, distances and relative orientations of the spin-carrying entities, for example, in the RC, are available from the dipolar part of this interaction. This method for structure determination is now being widely used for biological systems, together with site-directed

Wolfgang Lubitz (born 1949) studied chemistry and obtained his doctoral degree with Harry Kurreck and Klaus Möbius 1977 at the Freie Universität Berlin. After his habilitation (1982) he spent 2 years with George Feher (Physics Department, UC San Diego). After a short period as an associate professor of physics at the University of Stuttgart, he moved to the Technische Universität Berlin in 1991 as full professor of physical and biophysical chemistry. Since 2000 he has been scientific member of the Max Planck Society and director at the Institute of Radiation Chemistry in Mülheim/Ruhr.

Friedhelm Lendzian (born 1951) studied physics and chemistry in Tübingen, Heidelberg and Berlin and received his doctoral degree with Klaus Möbius at the Freie Universität Berlin in 1982. He worked as a postdoc and researcher at the Freie Universität Berlin before he moved to the Max-Volmer-Institute of the Technische Universität Berlin as a senior staff research scientist in 1992.

Robert Bittl (born 1959) studied physics at the Technische Universität München and received his doctoral degree 1988 with Klaus Schulten, whom he followed for a short period as a postdoc to Urbana, IL. After 2 years of postdoctoral work with Gerd Kothe at the Universität Stuttgart, he joined the Technische Universität Berlin in 1991 where he finished his habilitation in 1997. Since 2001, he has been professor of physics at the Freie Universität Berlin.

† Max-Planck-Institute für Strahlenchemie.
‡ Technische Universität Berlin.
§ Freie Universität Berlin.

10.1021/ar000084g CCC: $22.00 © 2002 American Chemical Society
Published on Web 05/01/2002

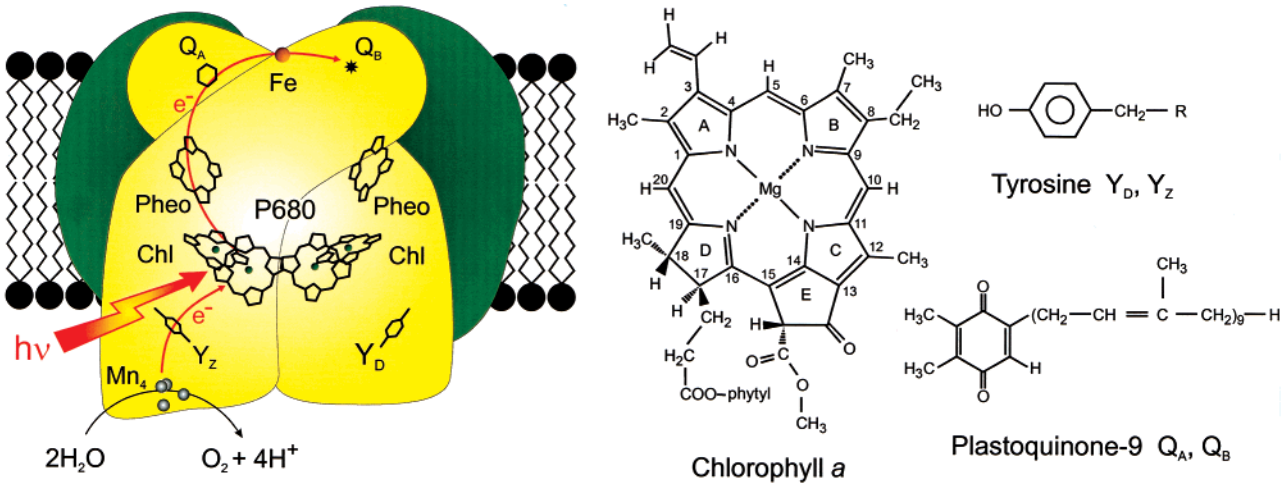

FIGURE 1. Schematic structure of PS II;[5] cofactors (P680 primary donor: pair of Chl *a* molecules; 2 monomeric Chl *a* and 2 Pheo *a*; Q_A,Q_B: 2 plastoquinone-9 molecules) are arranged in two branches related by a pseudo C_2 axis running through P680 and Fe^{2+}. Light-induced ET proceeds via one pigment branch as indicated. $P680^{+\bullet}$ withdraws an electron via tyrosine Y_Z from a tetranuclear manganese cluster, the locus of water oxidation. Right: structures of PS II cofactors; bacteriochlorophyll (BChl) *a* has a 3-acetyl group and hydrogenated ring B. (B)Pheo is the free base of (B)Chl.

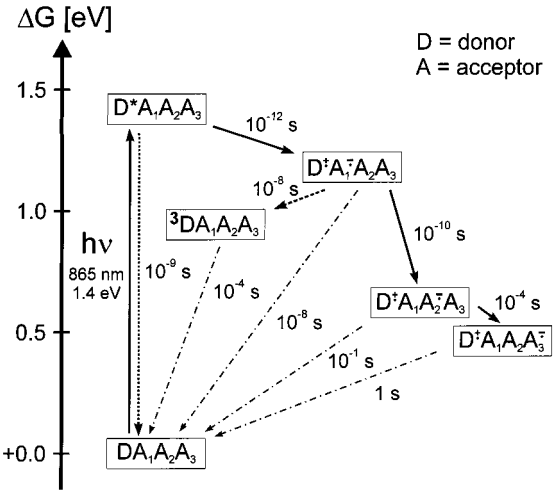

FIGURE 2. ET reactions and intermediate states in the RC on a free energy scale. Approximate ET times for purple bacteria (*Rb. sphaeroides*) and donor triplet formation (with prereduced quinone acceptors A_2/A_3) are given.[6,7]

spin-labeling techniques.[13] Furthermore, the exchange part of the interaction yields information on the extent of the electronic overlap.[14]

The hyperfine interaction between the unpaired electron and magnetic nuclei of the radical or of its immediate surrounding is usually very small and not resolved in the EPR spectra. Therefore, electron−nuclear double and triple resonance (ENDOR/TRIPLE)[15] or pulse EPR techniques, such as ESEEM,[16] must be employed to measure this interaction. The obtained hyperfine tensors comprise two contributions: the isotropic hyperfine couplings (hfcs) yield information about the unpaired spin density distribution over the molecule, whereas the anisotropic (dipolar) hfcs contain additional geometrical information. Furthermore, the nuclear quadrupole couplings are available for nuclei with spin $I > 1/2$.

The photogenerated radical pairs and triplet states in the RC often have lifetimes too short for standard cw EPR detection. Here, transient and pulse EPR[17] are used, which take advantage of signal enhancement due to spin polarization in these species and extend the accessible time range to a few tens of nanoseconds. Pulse ENDOR techniques[16] enable the detection of the hfcs of short-lived species, such as triplets or radical pairs having lifetimes in the microsecond range.

This information obtained from advanced EPR techniques on the electronic structure of the species involved in the RC, their interaction with the surrounding protein, with other cofactors, and their temperature-dependent dynamic behavior is of fundamental importance for understanding details of the ET. This brief review intends to show the relationship between EPR observables and the parameters that determine RC function for the radical ions, radical pairs, and triplet states that occur as intermediates in the RC.

II. Radical Ions

The radical ions created during ET in bacterial and plant RCs have been detected and characterized via their *g* factors and hfcs using cw EPR and ENDOR techniques (for references, see ref 10). Here, we will focus on the primary donor, D, that is located at the interface of exciton and electron transfer and acts as a highly optimized light-energy converter. Early EPR results showing that the cation radical $D^{+\bullet}$ is a (B)Chl dimer in bacterial RCs and PS I[18] were later supported by X-ray crystallographic data.[4,8] ENDOR experiments on native and isotopically labeled single crystals of bacterial RCs[19] yielded the spin-density distribution via the assigned hfcs and, together with molecular orbital calculations,[20] showed that $D^{+\bullet}$ ($P865^{+\bullet}$) is, indeed, a supermolecule with a wave function asymmetrically delocalized over both dimer halves.

An important question is why nature has chosen a chlorophyll dimer to function as primary donor in most species. One obvious reason, following from the exciton

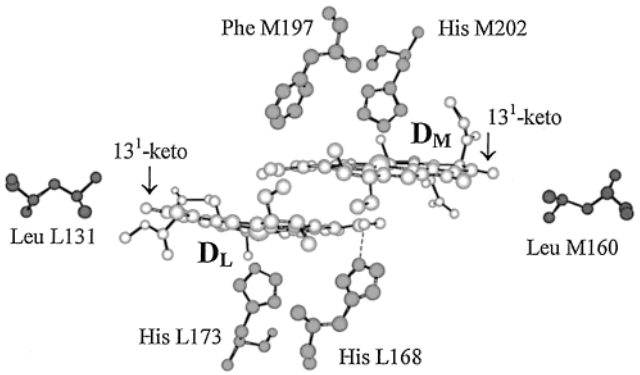

FIGURE 3. Structure of the primary donor (BChl *a* dimer, with halves D_L and D_M) in the RC of *Rb. sphaeroides*[4] with surrounding amino acids. Histidines M202 and L173 coordinate the 2 Mg ions, and His L168 forms a H-bond to the 3-acetyl group of D_L. Exchange of the other shown amino acids to His allows formation of H bonds to the remaining keto groups of the dimer (Table 1). L and M denote protein subunits of the RC.[4]

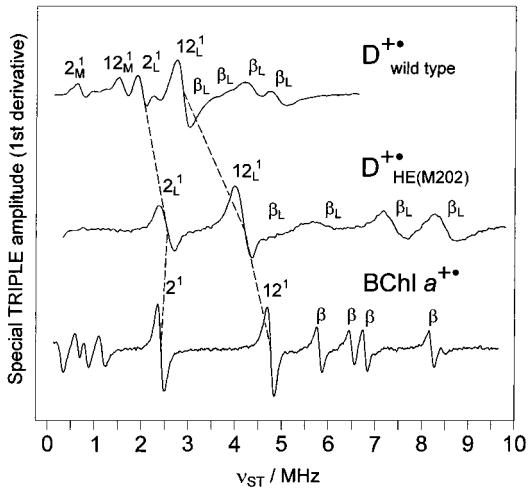

FIGURE 4. Special TRIPLE spectra of $D^{+\bullet}$ in *Rb. sphaeroides* wild type and mutant HE(M202) and of BChl $a^{+\bullet}$ in organic solvents, all in isotropic solution. The isotropic hyperfine couplings A_{iso} are directly obtained from the Special TRIPLE frequency by $\nu_{ST} = A_{iso}/2$ (for details, cf. refs 15 and 19).

transfer theory, is that a dimer can act as an efficient long wavelength trap for the light energy collected by the antenna system.[21] Furthermore, the donor initiates the fast activationless charge separation in the RC. To optimize this process and thereby maximize the ET rate, the redox potential of the donor must be tuned to an optimum value. Clearly, a dimer has more degress of freedom to achieve this by either structural changes of the individual dimer halves or the dimer structure itself. Furthermore, a broader range of interactions with the surrounding amino acids is possible, which can be specifically probed by employing site-directed mutagenesis.[7,22]

To monitor the impact of the protein on the electronic structure, the oxidation potential (E_D^{ox}), and the function of the dimer, specific amino acids have been changed in its surrounding. In one set of mutants of *Rhodobacter* (*Rb.*) *sphaeroides*, a histidine in the M subunit (His M202) that ligates the Mg atom of one of the dimer halves has been changed to other amino acids (Figure 3). Most residues do not significantly change E_D^{ox} (~500 mV in wild type) or the spin densities in the dimer. When, however, His is exchanged with the bulky Leu or Glu, E_D^{ox} attains a value close to that of monomeric BChl *a* in solution (~660 ± 10 mV).[23] ENDOR/TRIPLE further shows that the spin is completely localized on one BChl half (Figure 4). The pigment analysis shows that the RC contains three BChl and three BPheo, whereas four BChl and two BPheo are found in wild type. On the basis of earlier work,[24] it is therefore assumed that in these mutants, a BChl−BPheo "heterodimer" is the primary donor. Since BPheo has a higher redox potential than BChl,[23] only the BChl half is oxidized and carries the spin and positive charge. This situation is energetically less favorable than delocalization in a dimeric species, which leads to the observed increase of E_D^{ox}. For the heterodimer mutants, a lower quantum yield and reduced ET rates have been observed. The experiments clearly show that dimer formation alone significantly lowers and, thereby, adjusts the donor's oxidation potential.

Table 1. Spin Densities, Oxidation Potentials and ET Rates for Mutants Altering the Hydrogen Bonds to the Primary Donor in the RC of *Rb. sphaeroides*[22,25]

mutant strain	ρ_L[a]	n_H[b]	E_D^{ox}(mV)[c]	τ_{CD} (ns)[d]
HF(L168)	0.43	0	410	7730
LH(M160) + HF(L168)	0.70	1	485	1545
LH(L131) + HF(L168)	0.22	1	485	4820
wild type	0.68	1	505	960
HF(L168) + FH(M197)	0.41	1	545	1515
LH(M160)	0.83	2	565	345
LH(L131)	0.47	2	585	470
FH(M197)	0.65	2	630	185
LH(M160) + LH(L131)	0.69	3	635	210
LH(M160) + FM(M197)	0.83	3	700	130
LH(L131) + FM(M197)	0.40	3	710	165
LH(M160) + LH(131) + FH(M197)	0.80	4	765	80

[a] ρ_L, fraction of spin density on the dimer half D_L obtained from ENDOR/TRIPLE data.[25] [b] n_H, number of H bonds to carbonyl groups of the dimer. [c] E_D^{ox}, oxidation potential of the dimer vs NHE. [d] τ_{CD}, time constant for reduction of $D^{+\bullet}$ by cytochrome c_2^{2+}.[22]

In a second set of mutants of *Rb. sphaeroides*, hydrogen bonds have been broken or introduced between the carbonyl groups of the BChls of the dimer and the surrounding amino acid residues (Figure 3). Replacement of His L168 by Phe leads to an almost symmetric spin density distribution (Table 1). By exchanging other amino acids with histidines, H-bonds are formed to either dimer half, D_L or D_M (Figure 3), and the spin density can be shifted significantly from one to the other half. The dimer without any H bonds has a redox potential as low as ~400 mV. Each added H bond increases this value by ~50−100 mV. The species with 4 H bonds (triple mutant) reaches +765 mV.[22] Vibrational spectroscopy also indicates the formation of H bonds. The basic structure of the BChl dimer remains constant according to optical absorption spectroscopy.[22]

As expected from ET theory, the charge separation and charge recombination rates involving $D^{+\bullet}$ are all affected in the H bond mutants, although to different extent.[22] The

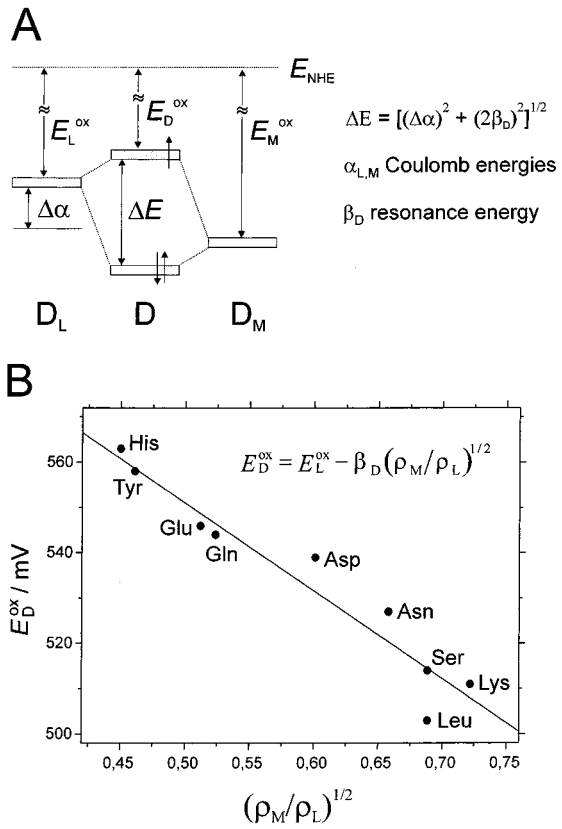

FIGURE 5. A. Molecular orbital scheme showing the highest occupied MO (HOMO) of the dimer D (center) and the 2 monomeric (B)Chl halves D_L and D_M. The vertical ionization potentials are related to the oxidation potentials shown (E_D^{ox}, E_L^{ox}, E_M^{ox}). H bonds to D_M or D_L will lower the energy of the respective half and change $\Delta\alpha$ and E_D^{ox}. B. Relationship between E_D^{ox} and the spin density ratio $(\rho_M/\rho_L)^{1/2}$ of the dimer for substitution of Leu M160 near D_M (Figure 4) to various H-bond-forming amino acids (see text and ref 26).

largest effect is observed for the reduction of $D^{+\bullet}$ by cyt c^{2+} ($CD^{+\bullet}A^{-\bullet} \rightarrow C^{+}DA^{-\bullet}$), where the time constant τ_{CD} changes by more than 2 orders of magnitude (Table 1). The ET rate is faster for all mutants with similar E_D^{ox} and the same n_H that have the electron spin—and thus also the "positive hole"—on D_L and slower when it is on D_M (see e.g. Table 1, rows 2 and 3), indicating a difference in distance or the electron tunneling pathway between the cyt *c* heme and the two dimer halves.[25]

The H-bond effect can be traced back to the electrostatic interaction between the oriented dipole of the H bond and the charge density and electron-spin distribution in the dimer.[26] A quantitative relationship between the oxidation potential of the donor and the electron-spin distribution can be derived on the basis of a simple molecular orbital (MO) scheme.[19] The energy-level diagram for the dimer and the two monomeric halves are shown in Figure 5A. The energy difference between the MOs of the dimer, ΔE, contains the Coulomb integral, $\Delta\alpha$, and the resonance integral, β_D. Removal of an electron from the upper dimer orbital yields the radical cation. The electron spin (and hole) distribution in the dimer, denoted by the ratio ρ_M/ρ_L, is then related to $\Delta\alpha$ and β_D (Figure 5).

In this simple model, the oxidation potential of the monomeric halves of the dimer is equal to the energy required to remove an electron from the HOMO of D_L (E_L^{ox}) or D_M (E_M^{ox}) or the HOMO of the dimer (E_D^{ox}). For a series of mutants in which, for example, the H-bond strength to the 13^1-keto group of D_M (residue M160) is altered (Figure 3), we expect that E_M^{ox} is predominantly changed and, to first order, E_L^{ox} remains constant. The simple model predicts a linear dependence of E_D^{ox} on $(\rho_M/\rho_L)^{1/2}$. Figure 5B, indeed, shows an approximately linear relationship. A linear fit yields $E_L^{ox} = 650$ meV and $\beta_D \approx 195$ meV. The value for E_L^{ox} is close to that of monomeric BChl *a*, and β_D is within a range expected from other results.[26] The strength of the effect of the different amino acid substitutions on oxidation potential and electron distribution follows the sequence His > Tyr > Glu > Gln > Asp > Asn > Ser > Lys (see Figure 5).[26]

The primary donors in PS II and in PS I contain Chl *a* that has a higher oxidation potential than BChl *a* (~660 mV), ranging from 740 to 930 mV, depending on the solvent.[23] The primary donor in PS II (P680) has a very high E_D^{ox} ($\geq +1.1$ V), sufficient to oxidize tyrosine, water, and other Chl's (see Figure 1). Since the formation of a dimer would decrease the oxidation potential, this species should clearly be a Chl *a* monomer in a hydrophobic pocket, which could increase E_D^{ox} easily to +1 V. A tight H bond to the 13^1-carbonyl group could add ~100 mV to this value. The recent X-ray structure of PS II[5], indeed, confirms that there are no strongly coupled chlorophylls in the RC (distance of cofactors $\geq$ 10 Å) (Figure 1). This agrees with studies of the primary donor cation radical $P680^{+\bullet}$,[27] which postulate that this species has a spin density distribution similar to that of monomeric Chl $a^{+\bullet}$.

The primary donor in PS I (P700) has an extremely low oxidation potential for a Chl *a* species ($\leq +0.5$ V). This indicates a dimeric species that was, indeed, found in the recent X-ray crystallographic structure[8] and was also derived from spectroscopic investigations, although the spin distribution in the cation radical $P700^{+\bullet}$ is more asymmetric than in the bacterial case.[28,29] However, in PS I it must be assumed that the type and local structure of the pigments[8] also play an important role in adjusting the redox potential (see ref 29).

III. Triplet States

Chlorophyll and bacteriochlorophyll molecules form triplet states ($S = 1$) upon photoexcitation that are populated with high yield from the excited singlet state by intersystem crossing on a nanosecond time scale and have lifetimes of 0.1 to 1 ms.[12] Such triplet states are of potential danger for all photosystems, since they react with molecular oxygen generating singlet oxygen, which is extremely aggressive and leads to damaging photooxidation reactions. Chlorophyll triplet states are, therefore, carefully avoided in all photosystems. This is achieved by fast singlet energy transfer on a subpicosecond time scale in the antennae[21] and by fast charge separation on the picosecond time scale in the RC.[6]

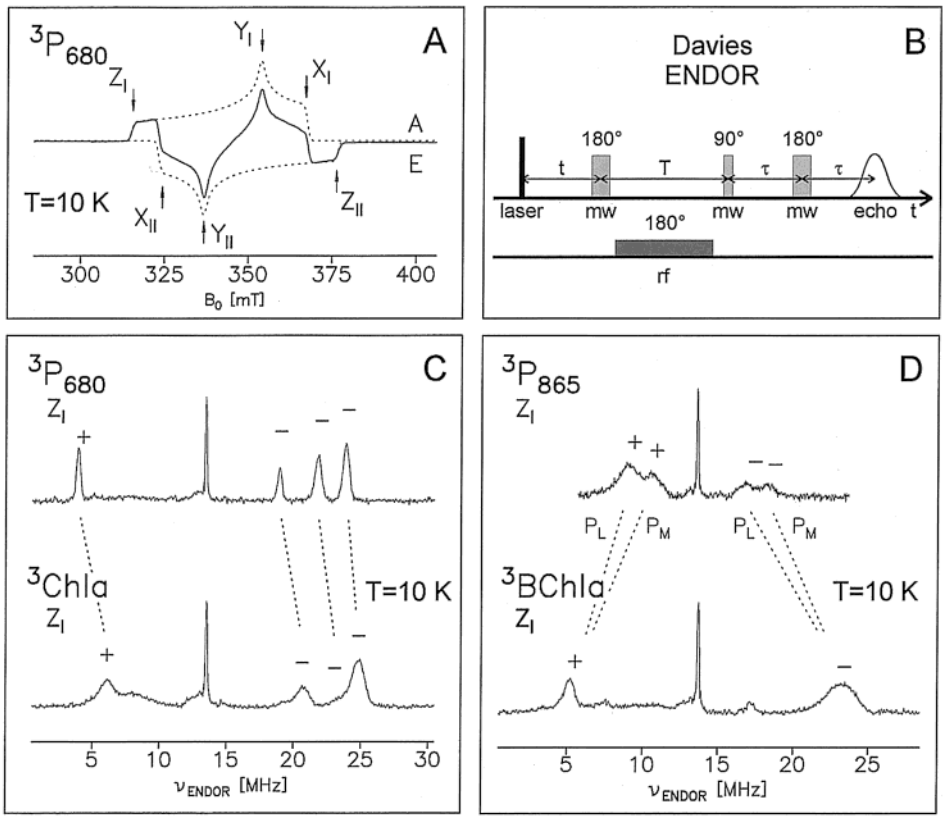

FIGURE 6. **A**. Transient EPR spectrum of ^{3}P680 in frozen solution of a PS II (D1D2 cyt b559) preparation recorded 1 μs after repetitive pulse laser excitations showing absorption (A) and emission (E) lines. **B**. Pulse sequence used for ENDOR experiments. **C**. Pulse ENDOR spectra of ^{3}P680 in PS II and ^{3}Chl *a* in frozen solution at EPR field position Z_I. Signs of hfcs are indicated. **D**. Pulse ENDOR spectra for ^{3}P865 of bacterial RCs (*Rb. sphaeroides*) and ^{3}BChl *a* in frozen solution.[37]

Additionally, nature has provided protection by incorporating carotenoids (Car) in the antenna systems and the RCs in close contact with chlorophyll molecules, thereby enabling efficient triplet energy transfer from chlorophyll to Car.[30] Car triplet states are too low in energy to create singlet oxygen in a reaction with molecular oxygen. Instead, they decay by internal conversion to the ground state.[30] Chl/Car triplet energy transfer has been investigated by transient optical absorption in all photosystems and by EPR spectroscopy in bacterial light-harvesting antenna complexes,[31] as well as in reaction centers,[12,32] and was shown to be an effective process at ambient temperatures, where photosynthesis occurs in vivo. This process is, however, slowed at low temperature.

When forward electron transfer to the secondary quinone acceptors in RCs is blocked, charge recombination from the primary radical pair $D^{+\bullet}A_1^{-\bullet}$ leads to formation of the triplet state of the primary donor, ^{3}D (Figure 2). Although ^{3}D is not a functional state in the ET process, its investigation is important to understand the primary donor excited-state electronic properties and the triplet energy transfer from Chl to Car.

The interaction between the two unpaired spins in the highest occupied (HOMO) and lowest unoccupied (LUMO) molecular orbital of ^{3}D (total spin $S = 1$) leads to zero field splitting, described by the parameters D and E, which reflect the size and symmetry of the two singly occupied orbitals. D and E can advantageously be measured in the absence of a magnetic field by optically detected magnetic resonance (ODMR).[9,10]

If the charge recombination generating ^{3}D proceeds in a magnetic field, of the three high-field triplet sublevels (T_+, T_0, T_-) only one (T_0) is populated, leading to strong emission and absorption signals in the observed EPR spectra[12] that can be detected with a time resolution of several tens of nanoseconds[17] by time-resolved transient EPR techniques.

The triplet states ^{3}D in plant PS I (^{3}P700) and PS II (^{3}P680) have been investigated by transient EPR over a wide temperature range (10−298 K) and compared with ^{3}Chl *a* in organic solvent. From a change of the observed E value (asymmetry parameter of the triplet wave function), it has been suggested that the triplet excitation is localized on one chlorophyll molecule at low temperature but delocalized onto a second chlorophyll molecule at higher temperature in both photosystems.[33,34]

Orientation-dependent EPR studies have been performed on ^{3}D in single crystals of bacterial RCs. Comparison of the obtained data with the X-ray structure of the primary donor yielded the orientation of the triplet symmetry axes in a molecular frame, from which a delocalized dimeric state ^{3}D was concluded.[35] Transient EPR studies performed on ^{3}P680 in PS II particles oriented on Mylar sheets led to the proposal that ^{3}P680 is localized on one single accessory chlorophyll (Chl in Figure 1)[36] and not on a chlorophyll of the dimeric primary donor P680.

This could be due to the unusual orbital energies of P680 that result in the large redox potential of P680/P680$^{+\bullet}$.

The zero field splitting parameters *D* and *E* obtained by ODMR and EPR are integral properties of the triplet wave functions. More detailed information can be obtained by determining the hfcs of specific nuclei in ^{3}D, which reflect the electron spin density at the respective nucleus and can be resolved by ENDOR experiments. Pulsed laser excitation (10-ns pulse width) was used to generate ^{3}D at low temperatures with high yield, and strong spin polarization gave rise to intense EPR signals showing absorption and emission peaks (see Figure 6A). Pulse ENDOR experiments were recorded in a time window of a few microseconds after generation of the excited triplet state (Figure 6B). The resulting resolution in the ENDOR spectra is under these conditions close to the physical limit given by the lifetime broadening of the triplet spin energy levels.

Hyperfine couplings were measured for ^{3}D of the photosynthetic bacterium *Rb. sphaeroides* (^{3}P865) by pulse ENDOR using repetitive laser flash excitation (Figure 6D).[37] Comparison with the spectra of ^{3}BChl *a* in a frozen organic solvent showed a significant reduction of the hfcs in ^{3}P865 and a splitting of the ENDOR lines (see Figure 6D). The detailed analysis led to an assignment of the couplings to specific nuclei and also allowed distinguishing between spin density in the HOMO or LUMO orbitals. The results clearly showed an asymmetric delocalization of the triplet excitation over the two BChl *a* molecules constituting ^{3}P865 with a significant charge transfer contribution (~20%), presumably in favor of $D_L^+D_M^-$.[37]

ENDOR experiments were also performed on ^{3}P680 in plant PS II (Figure 6C;[38] see also ref 39). Comparison of the pulse ENDOR spectra of ^{3}P680 and ^{3}Chl *a* in frozen solvent showed no significant reduction of hyperfine splittings in ^{3}P680.[38] This confirmed earlier conclusions based on EPR[36] that the triplet excitation in PS II is localized on *one* chlorophyll molecule (at $T = 10$ K). The small shifts of the hyperfine couplings of ^{3}P680, compared with ^{3}Chl *a*, indicate specific interactions with the protein that are likely to also influence orbital energies and redox potentials of the molecule.

IV. Radical Pairs

During the ET processes in the photosystems, most radical ions are created as radical ion pairs (Figure 2). The interaction between the two unpaired electrons can be used to obtain structural and functional information. This approach is similar to the site-directed spin-labeling technique by which structural information on proteins is obtained.[13] Thereby, the $1/r^3$ dependence of the dipolar spin−spin interaction is mainly used as a source of structural information. The photosystems provide the essential advantage that the paramagnetic states occur naturally and do not require artifical insertion of spin labels.[17]

We have utilized this approach to study by multifrequency EPR a functional state with two unpaired electrons in bacterial RCs, with one electron on each of the two quinone acceptors ($Q_A^{-\bullet}Q_B^{-\bullet}$). The analysis of the dipolar spin−spin coupling showed that the geometry of this functional state is in very good agreement with the X-ray structure obtained under illumination ($Q_AQ_B^{-\bullet}$ state).[14] This implies that Q_A does not undergo any significant structural changes upon reduction in contrast to Q_B.[40] The analysis also gave an estimate for the exchange interaction *J* between the two electron spins, which is related to the ET rate between $Q_A^{-\bullet}$ and $Q_B^{-\bullet}$ and allows an analysis of the ET efficiency between the two cofactors. It was concluded that the protein between Q_A and Q_B is a better electron conductor than the average found in a wide variety of proteins.[41]

Using time-resolved EPR, it is possible to take advantage of the fact that in the function of RCs, several states with two unpaired electron spins that are accessible to this technique occur as transient intermediates on a microsecond to millisecond time scale. Structural information can, thus, be obtained directly on active states of the protein. For systems with a structure known from X-ray crystallography, this is used to investigate structural changes during protein function. For systems with unknown structure, the active-state structure can serve as a starting model for the ground state. Using transient EPR, the latter possibility has initially been mainly exploited to investigate the sufficiently long-lived $D^{+\bullet}A_2^{-\bullet}$ states in RCs (Figure 2).[17]

The transient spin-polarized EPR spectra of these radical pairs are very sensitive to the relative orientation of the two spin-carrying cofactors due to the anisotropy of the electron spin−spin interaction and of the *g* tensors but are rather insensitive to the distance between the cofactors. As proposed in a theoretical study,[42] the distance-dependence of the electronic spin−spin coupling is, however, accessible by pulse EPR on the light-induced charge-separated states in RCs using a two-pulse electron spin−echo envelope modulation (out-of-phase ESEEM) experiment. Experimentally, this has been first shown for $P865^{+\bullet}Q_A^{-\bullet}$[43] in RCs from *Rb. sphaeroides* with known distance of the cofactors in the ground state.

An interesting application of this technique to bacterial RCs has been the investigation of structural changes as a consequence of the light-induced electron transfer.[44] Using time-resolved EPR, the kinetic differences observed originally by transient absorbance difference spectroscopy for samples frozen in the charge-separated and in the ground state could be confirmed.[45] However, the respective ESEEM experiments (Figure 7) did not reveal a significant alteration in the cofactor distance in these states (error, ±0.3 Å).[45] A likely alternative explanation for the modified ET kinetics is changes of the reorganization energy in the different states.

In PS I, time-resolved EPR on the charge-separated state $P700^{+\bullet}Q_K^{-\bullet}$ in frozen solution and single crystals has been mainly aimed at establishing the exact position and orientation of the phylloquinone acceptor Q_K (Figure

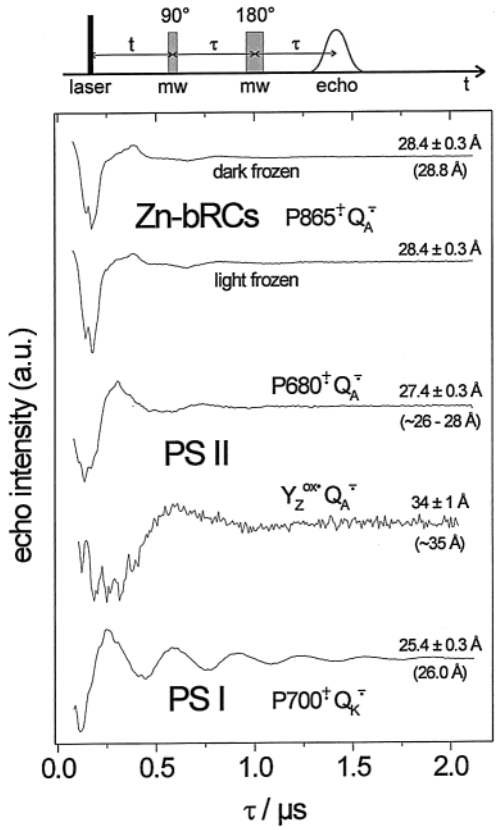

FIGURE 7. Electron spin−echo modulation due to the electron spin−spin interaction for various radical pair states in the photosystems: $P865^{+\bullet}QA^{-\bullet}$ in Zn-substituted RCs of *Rb. sphaeroides* frozen in the dark and in the light,[45] $P680^{+\bullet}Q_A^{-\bullet}$ and $Y_Z^{ox}Q_A^{-\bullet}$ in PS II from spinach,[48,49] $P700^{+\bullet}Q_K^{-\bullet}$ in PS I from *Synechococcus elongatus*;[47] PS II experiments at $T \cong 290$ K; all others at 80 K. Distances evaluated from the modulation frequencies are compared with those from X-ray crystallography[4,5,8,40] (in brackets). Top: pulse sequence used.

7).[46,47] Time-resolved EPR studies on transient species involved in the primary charge transfer process in PS II are of particular interest, since the mechanism of charge separation is not yet fully understood. In one model, ET starts from the excited state P680* and proceeds probably via the monomeric Chl and Pheo to the quinone acceptors as in bacterial RCs (Figure 1). In another scenario, the initial charge separation takes place between the accessory Chl and Pheo. Indirect evidence for the involvement of the "accessory" Chl comes from the finding that at low temperatures, this species carries the triplet exciton (see above).[36] Here, pulse EPR using liquid solutions of PS II allowed monitoring the consecutive radical pair states $P680^{+\bullet}Q_A^{-\bullet}$[48] and $Y_Z^{ox}Q_A^{-\bullet}$[49] by variation of the delay between the laser flash, inducing the ET process, and the EPR detection sequence (see Figure 7). Analysis of the time-dependence of the ESEEM resulted in a distance between $P680^{+\bullet}$ and $Q_A^{-\bullet}$ of 27.4 ± 0.4 Å and Y_Z^{ox} and $Q_A^{-\bullet}$ of 34 ± 1 Å. These distances are in very good agreement with the tentative assignment of Q_A and Y_Z in the present X-ray model of PS II (Figure 1).[5] For $P680^{+\bullet}Q_A^{-\bullet}$, an almost identical distance has been found in a study on frozen solutions.[50] This distance is compatible only with an assignment of the species $P680^{+\bullet}$ to one of the two Chl's with planes perpendicular to the membrane plane (see Figure 1). A distinction between the two molecules on the basis of their distance to Q_A is not yet possible. However, the "accessory" Chl *a*, where the P680 triplet state seems to be localized at low temperatures, can be excluded as the oxidized species $P680^{+\bullet}$, at least on the time scale of our experiment (approximately 0.2−1 μs). The localization of the triplet state on a chromophore different from the one carrying the positive charge seems to be a distinguishing feature between purple bacterial RCs and PS II both belonging to the type II RCs.

A promising extension of EPR spectroscopy to study the interesting species $P680^{+\bullet}$ is pulse ENDOR spectroscopy on short-lived radical pair species. We have established this technique and applied it to PS I.[47] Further progess with this method will enable studies of $P680^{+\bullet}$ without the requirement to chemically stabilize this extremely reactive species.

V. Conclusions

Advanced EPR techniques proved to be very useful to probe distances, geometries and valence electron distributions of paramagnetic intermediates in photosynthetic proteins with nanosecond to microsecond time resolution. This information is important for understanding details of the ET process in photosynthesis. The methods have great potential for investigating other biological systems in which radicals, radical pairs, triplet states, or transition metal centers are present and play a structural or functional role.

The authors thank all collaborators, students, and colleagues who contributed to this work and whose names are given in the references. This work was supported by Deutsche Forschungsgemeinschaft (Sfb 498), European Union (FMRX-CT98-0214) and Fonds der Chemischen Industrie.

References

(1) *Advances in Photosynthesis*; Govindjee, Ed.; Kluwer Academic Publishers: Dordrecht, 1995−2001; Book Series Vols. 1−11.
(2) Blankenship, R. E.; Madigan, M. T.; Bauer, C. E., Eds. *Anoxygenic Photosynthetic Bacteria*; Kluwer Academic Publishers: Dordrecht, 1995.
(3) Ort, D. R.; Yocum, C. F., Eds. *Advances in Photosynthesis. Oxygenic Photosynthesis: The Light Reactions*; Kluwer Academic Publishers: Dordrecht, 1996.
(4) Lancaster, C. R. D.; Ermler, U.; Michel, H. The Structure of Photosynthetic Reaction Centers from Purple Bacteria as Revealed by X-ray Crystallography. In *Anoxygenic Photosynthetic Bacteria*; Blankenship, R. E., Madigan, M. T., Bauer, C. E., Eds.; Kluwer Academic Publishers: Dordrecht, 1995; pp 503−526.
(5) Zouni, A.; Witt, H. T.; Kern, J.; Fromme, P.; Krauss, N.; Saenger, W.; Orth, P. Crystal structure of photosystem II from *Synechococcus elongatus* at 3.8 Å resolution. *Nature* **2001**, *409*, 739−743.
(6) Woodbury, N. W.; Allen, J. P. The Pathway, Kinetics and Thermodynamics of Electron Transfer in Wild-Type and Mutant Reaction Centers of Purple Nonsulfur Bacteria. In *Anoxygenic Photosynthetic Bacteria*; Blankenship, R. E., Madigan, M. T., Bauer, C. E., Eds.; Kluwer Academic Publishers: Dordrecht, 1995; pp 527−557.
(7) van Brederode, M. E.; Jones, M. R. Reaction Centers of Purple Bacteria. In *Subcellular Biochemistry, Enzyme-Catalyzed Electron and Radical Transfer*; Holzenburg, Scrutton, Eds.; Kluwer Academic/Plenum Press: New York, 2000; Vol. 35; pp 621−676.

(8) Jordan, P.; Fromme, P.; Witt, H. T.; Klukas, O.; Saenger, W.; Krauss, N. Three-dimensional structure of cyanobacterial photosystem I at 2.5 Å resolution. *Nature* **2001**, *411*, 909−917.

(9) Amesz, J.; Hoff, A. J. Biophysical Techniques in Photosynthesis. In *Advances in Photosynthesis*; Govindjee, Ed.; Vol. 3, Part 2, Magnetic Resonance; Kluwer Academic Publishers: Dordrecht, 1996.

(10) Hoff, A. J.; Deisenhofer, J. Photophysics of Photosynthesis. Structure and Spectroscopy of Reaction Centers of Purple Bacteria. *Phys. Rep.* **1997**, *287*, 1−248.

(11) Möbius, K. Primary processes in photosynthesis: what do we learn from high-field EPR spectroscopy? *Chem. Soc. Rev.* **2000**, *29*, 129−139.

(12) Budil, D. E.; Thurnauer, M. C. The Chlorophyll Triplet State as a Probe of Structure and Function in Photosynthesis. *Biochim. Biophys. Acta* **1991**, *1057*, 1−41.

(13) Berliner, L. J., Ed. Spin Labeling. The Next Millennium. In *Biological Magnetic Resonance*; Plenum Press: New York, 1998; Vol. 14.

(14) Calvo, R.; Abresch, E. C.; Bittl, R.; Feher, G.; Hofbauer, W.; Isaacson, R. A.; Lubitz, W.; Okamura, M. Y.; Paddock, M. L. EPR Study of the Molecular and Electronic Structure of the Semiquinone Biradical $Q_A^{-\bullet}Q_B^{-\bullet}$ in Photosynthetic Reaction Centers from *Rb. sphaeroides*. *J. Am. Chem. Soc.* **2000**, *122*, 7327−7341.

(15) Lubitz, W.; Lendzian, F. ENDOR Spectroscopy. In *Biophysical Techniques in Photosynthesis*; Amesz, J., Hoff, A. J., Eds.; Kluwer Academic Publishers: Dordrecht, 1996; pp 255−275.

(16) Schweiger, A.; Jeschke, G. *Principles of Pulse Electron Paramagnetic Resonance*; Oxford University Press: New York, 2001.

(17) Stehlik, D.; Möbius, K. New EPR Methods for Investigating Photoprocesses with Paramagnetic Intermediates. *Annu. Rev. Phys. Chem.* **1997**, *48*, 745−784.

(18) Norris, J. R.; Uphaus, R. A.; Crespi, H. L.; Katz, J. J. Electron Spin Resonance of Chlorophyll and the Origin of Signal I in Photosynthesis. *Proc. Natl. Acad. Sci. U.S.A.* **1971**, *68*, 625−628.

(19) Lendzian, F.; Huber, M.; Isaacson, R. A.; Endeward, B.; Plato, M.; Bönigk, B.; Möbius, K.; Lubitz, W.; Feher, G. The Electronic Structure of the Primary Donor Cation Radical in *Rhodobacter sphaeroides* R-26: ENDOR and TRIPLE Resonance Studies in Single Crystals of Reaction Centers. *Biochim. Biophys. Acta* **1993**, *1183*, 139−160.

(20) Plato, M.; Möbius, K.; Lubitz, W. Molecular Orbital Calculations on Chlorophyll Radical Ions. In *Chlorophylls*; Scheer, H., Ed.; CRC Press: Boca Raton, FL, 1991; pp 1015−1046.

(21) van Amerongen, H.; Valkunas, L.; van Grondelle, R. *Photosynthetic Excitons*; World Scientific Publishing: Singapore, 2000.

(22) Allen, J. P.; Williams, J. C. Relationship between the oxidation potential of the bacteriochlorophyll dimer and electron transfer in photosynthetic reaction centers. *J. Bioenerg. Biomembr.* **1995**, *27*, 275−283.

(23) Watanabe, T.; Kobayashi, M. Electrochemistry of Chlorophylls. In *Chlorophylls*; Scheer, H., Ed.; CRC Press: Boca Raton, FL, 1991; pp 287−364.

(24) McDowell, L. M.; Gaul, D.; Kirmaier, C.; Holten, D.; Schenck, C. C. Investigation into the Source of Electron-Transfer Asymmetry in Bacterial Reaction Centers. *Biochemistry* **1991**, *30*, 8315−8322.

(25) Rautter, J.; Lendzian, F.; Lin, X.; Williams, J. C.; Allen, J. P.; Lubitz, W. Effect of Orbital Asymmetry in $P^{+\bullet}$ on Electron Transfer in Reaction Centers of *Rb. sphaeroides*. In *The Reaction Center of Photosynthetic Bacteria, Structure and Dynamics*; Michel-Beyerle, M.-E., Ed.; Springer: Berlin, 1996; pp 37−50.

(26) Müh, F.; Lendzian, F.; Roy, M.; Williams, J. C.; Allen, J. P.; Lubitz, W. Pigment−Protein Interactions in Bacterial Reaction Centers and their Influence on Oxidation Potential and Spin Density Distribution of the Primary Donor. *J. Phys. Chem. B* **2002**, *106*, 3226−3236.

(27) Rigby, S. E. J.; Nugent, J. H. A.; O'Malley, P. J. ENDOR and Special Triple Resonance Studies of Chlorophyll Cation Radicals in Photosystem 2. *Biochemistry* **1994**, *33*, 10043−10050.

(28) Käss, H.; Fromme, P.; Witt, H. T.; Lubitz, W. Orientation and Electronic Structure of the Primary Donor Radical Cation $P700^{+\bullet}$ in Photosystem I: A Single Crystals EPR and ENDOR Study. *J. Phys. Chem. B* **2001**, *105*, 1225−1239.

(29) Webber, A. N.; Lubitz, W. P700: The Primay Electron Donor of Photosystem I. *Biochim. Biophys. Acta* **2001**, *1507*, 61−79.

(30) Cogdell, R. J.; Howard, T. D.; Bittl, R.; Schlodder, E.; Geisenheimer, I.; Lubitz, W. How Carotenoids Protect Bacterial Photosynthesis. *Philos. Trans. R. Soc. London B* **2000**, *355*, 1345−1349.

(31) Bittl, R.; Schlodder, E.; Geisenheimer, I.; Lubitz, W.; Cogdell, R. J. Transient EPR and Absorption Studies of Carotenoid Triplet Formation in Purple Bacterial Antenna Complexes. *J. Phys. Chem. B* **2001**, *105*, 5525−5535.

(32) deWinter, A.; Boxer, S. G. The Mechanism of Triplet Energy Transfer from the Special Pair to the Carotenoid in Bacterial Photosynthetic Reaction Centers. *J. Phys. Chem. B* **1999**, *103*, 8786−8789.

(33) Sieckmann, I.; Brettel, K.; Bock, C.; van der Est, A.; Stehlik, D. Transient Electron Paramagnetic Resonance of the Triplet State of P700 in Photosystem I: Evidence for Triplet Delocalization at Room Temperature. *Biochemistry* **1993**, *32*, 4842−4847.

(34) Kamlowski, A.; Frankemöller, L.; van der Est, A.; Stehlik, D. Evidence for Delocalization of the Triplet State $^3P_{680}$ in the D_1D_2-cytb_{559}−Complex of Photosystem II. *Ber. Bunsen-Ges. Phys. Chem.* **1996**, *100*, 2045−2051.

(35) Norris, J. R.; Budil, D. E.; Gast, P.; Chang, C.-H.; El-Kabbani, O.; Schiffer, M. Correlation of Paramagnetic States and Molecular Structure in Bacterial Photosynthetic Reaction Centers: The symmetry of the primary electron donor in *Rhodopseudomonas viridis* and *Rhodobacter sphaeroides* R-26. *Proc. Natl. Acad. Sci. U.S.A.* **1989**, *86*, 4335−4339.

(36) van Mieghem, F. J. E.; Satoh, K.; Rutherford, A. W. A Chlorophyll Tilted 30° Relative to the Membrane in the Photosystem II Reaction Centre. *Biochim. Biophys. Acta* **1991**, *1058*, 379−385.

(37) Lendzian, F.; Bittl, R.; Lubitz, W. Pulsed ENDOR of the Photoexcited Triplet States of Bacteriochlorophyll *a* and of the Primary Donor P865 in Reaction Centers of *Rhodobacter sphaeroides* R-26. *Photosyn. Res.* **1998**, *55*, 189−197.

(38) Lendzian, F.; Bittl, R.; Telfer, A.; Barber, J.; Lubitz, W. Time-Resolved ENDOR of the Triplet State of P680 in PS II Reaction Centers. In *Photosynthesis: Mechanisms and Effects*; Garab, G., Ed.; Kluwer Academic Publishers: Dordrecht, 1998; Vol. II.; pp 1057−1060.

(39) Di Valentin, M.; Kay, C. W. M.; Giacometti, G.; Möbius, K. A Time-Resolved Electron Nuclear Double Resonance Study of the Photoexcited Triplet State of P680 in Isolated Reaction Centers of Photosystem II. *Chem. Phys. Lett.* **1996**, *248*, 434−441.

(40) Stowell, M. H. B.; McPhillips, T. M.; Rees, D. C.; Soltis, S. M.; Abresch, E.; Feher, G. Light-Induced Structural Changes in Photosynthetic Reaction Center: Implications for Mechanism of Electron−Proton Transfer. *Science* **1997**, *276*, 812−816.

(41) Page, C. C.; Moser, C. C.; Chen, X.; Dutton, P. L. Natural Engineering Principles of Electron Tunneling in Biological Oxidation−Reduction. *Nature* **1999**, *402*, 47−52.

(42) Salikhov, K. M.; Kandrashkin, Y. E.; Salikhov, A. K. Peculiarities of Free Induction and Primary Spin−Echo Signals for Spin-Correlated Radical Pairs. *Appl. Magn. Res.* **1992**, *3*, 199−216.

(43) Dzuba, S. A.; Gast, P.; Hoff, A. J. ESEEM study of spin−spin interactions in spin-polarized $P^+Q_A^-$ pairs in the photosynthetic purple bacterium *Rhodobacter sphaeroides* R26. *Chem. Phys. Lett.* **1995**, *236*, 595−602.

(44) Kleinfeld, D.; Okamura, M. Y.; Feher, G. Electron-transfer kinetics in photosynthetic reaction centers cooled to cryogenic temperatures in the charge-separated state: evidence for light-induced structural changes. *Biochemistry* **1984**, *23*, 5780−5786.

(45) Zech, S.; Bittl, R.; Gardiner, A.; Lubitz, W. Transient and Pulsed EPR Spectroscopy on the Radical Pair State $P865^{+\bullet}$ $Q_A^{-\bullet}$ to Study Light-Induced Structural Changes in Bacterial Reaction Centers. *Appl. Magn. Res.* **1997**, *13*, 517−529.

(46) Bittl, R.; Zech, S.; Fromme, P.; Witt, H. T.; Lubitz, W. Pulsed EPR Structure Analysis of Photosystem I Single Crystals: Localization of the Phylloquinone Acceptor. *Biochemistry* **1997**, *36*, 12001−12004.

(47) Bittl, R.; Zech, S. G. Pulsed EPR Spectroscopy on Short-Lived Intermediates in Photosystem I. *Biochim. Biophys. Acta* **2001**, *1507*, 194−211.

(48) Zech, S. G.; Kurreck, J.; Eckert, H.-J.; Renger, G.; Lubitz, W.; Bittl, R. Pulsed EPR Measurement of the Distance between $P680^{+\cdot}$ and $Q_A^{-\bullet}$ in Photosystem II. *FEBS. Lett.* **1997**, *414*, 454−456.

(49) Zech, S. G.; Kurreck, J.; Renger, G.; Lubitz, W.; Bittl, R. Determination of the Distance between Y_Z^{ox} and $Q_A^{-\bullet}$ in Photosystem II by Pulsed EPR Spectroscopy on Light-Induced Radical Pairs. *FEBS Lett.* **1999**, *442*, 79−82.

(50) Hara, H.; Dzuba, S. A.; Kawamori, A.; Akabori, K.; Tomo, T.; Satoh, K.; Iwaki, M.; Itoh, S. The distance between P680 and Q_A in photosystem II determined by ESEEM spectroscopy. *Biochim. Biophys. Acta* **1997**, *1322*, 77−85.

AR000084G